

ELECTRO- AND PHOTONUCLEAR PHYSICS WITH POLARIZED BEAMS AND TARGETS

R. J. Holt

Physics Division, Argonne National Laboratory, Argonne IL 60439-4843 USA

ABSTRACT

Two long-standing issues in photonuclear physics, the giant M1 resonance in Pb and deuteron photodisintegration, have been studied recently with polarized photons at Urbana and Frascati, respectively. The implications that this work has for settling these key issues will be discussed. In addition, the advantages of the internal polarized target method for electron scattering studies will be discussed and the technology of internal polarized target development will be reviewed. The first results from a spin-exchange, optically-pumped polarized H and D source will be presented.

DEC 02 1987

CONF-8706232--1

DE88 003066

I. INTRODUCTION

It is now widely recognized that polarization methods in electromagnetic studies of nuclei are potentially a powerful technique. The internal polarized target technique which was discussed by Professor Popov in the previous paper¹ has led recently to many suggestions² for experiments and, in addition to the work in progress here at Novosibirsk, to proposals³ for electron rings and internal target facilities at the MIT-Bates Laboratory and NIKHEF. The primary difficulty with this method is generating the polarized target and I shall discuss some novel developments in this field. Two key experiments⁴ will be discussed as internal target experiments: (i) polarization in electron-deuteron scattering and (ii) the charge form factor of the neutron. The need for \vec{D} and $^3\vec{He}$ targets is emphasized for these experiments.

The submitted manuscript has been authorized by a contractor of the U. S. Government under contract No. W-31-109-ENG-38. Accordingly, the U. S. Government retains a nonexclusive, royalty-free license to publish or reproduce the published form of this contribution, or allow others to do so, for U. S. Government purposes.

JSW

Nuclear studies involving the use of polarized photons have burgeoned during the past few years owing to the development of the LADON Facility at the ADONE storage ring and the development of the selective residual-electron tagging technique at Urbana. In addition, the LEGS Facility at Brookhaven is expected to begin operation this Fall and provide tagged, polarized photon beams in the energy region of the delta resonance. Thus, I would like to highlight some initial findings from these new facilities.

II. GIANT M1 RESONANCE IN THE Pb REGION

The ^{208}Pb nucleus is expected to represent an ideal example of the collective M1 resonance since both the $1_{13/2}$ neutron and $h_{11/2}$ proton shells are filled while their spin-orbit partners are vacant. After substantial effort⁵ approximately one-third of the expected strength for the M1 isovector sum rule has been observed for ^{208}Pb . This result led to much quandary since the theoretical calculations, even with 2p-2h and Δ -h admixtures, could not account for such a large quenching of the M1 resonance. The primary difficulty with ^{208}Pb is that most of the M1 strength is expected to lie above the photoneutron threshold (7.4 MeV) where the experiments are exceedingly difficult. Laszewski et al. have pointed out that ^{206}Pb might be a better nucleus to search for the giant M1 resonance since the (γ, n) threshold is much higher (8.1 MeV), and resonance fluorescence methods with polarized photons would be a powerful method for identifying the spin, parity, and transition strengths of the resonances.

In order to perform the experiment, Laszewski et al.⁶ at Urbana have recently enhanced the polarization in bremsstrahlung production by selectively tagging the residual electron as indicated schematically in the upper part of Fig. 1. Since the photon tagging spectrometer at Urbana is double-focusing, a

fixed collimator was placed in the magnet gap in order to tag electrons slightly out of the bremsstrahlung production plane. This has the effect of enhancing the photon polarization by a large factor as shown by a comparison of the lower graphs of Fig. 1. This novel technique was applied⁷ successfully to search for the collective M1 excitation in ^{206}Pb . The results of this work are shown in the upper panel of Fig. 2. A $B(\text{M1}, \uparrow)$ of $19 \pm 2 \mu_0^2$ was found below 8 MeV and is consistent with the M1 sum rule⁸ for isovector transitions in Pb. This work clears up a long-standing puzzle in nuclear physics.

The presently known $B(\text{M1}, \uparrow)$ for excitations in ^{208}Pb are compared with that in ^{206}Pb in the lower panel of Fig. 2. Although the known M1 strength in ^{208}Pb is only $B(\text{M1}, \uparrow) \approx 7 \mu_0^2$, its distribution may be consistent with that in ^{206}Pb as suggested in Fig. 2. Thus, it is expected that further work will yield more M1 strength in ^{208}Pb and there will not be an anomalous quenching effect as previously suggested.

III. PHOTODISINTEGRATION OF THE DEUTERON

In recent years much progress has been made in the study of the $D(\gamma, n)p$ reaction owing to the development of new techniques which can yield high-accuracy results. The development of the Compton back-angle scattering facility⁹ (LADON) at Frascati has permitted measurement¹⁰ of the polarization-dependent component, $pI_1(\theta)$, of the $D(\gamma, n)p$ cross section. The differential cross section for the photodisintegration process with linearly polarized photons of polarization p is given by

$$\frac{d\sigma}{d\Omega} = I_0(\theta) + pI_1(\theta) \cos(\phi)$$

where I_0 is the cross section for unpolarized particles and ϕ is the azimuthal

angle between the reaction plane and the polarization plane of the incident photon. In terms of the Partovi coefficients¹¹ these cross sections are given by

$$I_0 = a + b \sin^2 \theta + c \cos \theta + d \sin^2 \theta \cos \theta + e \sin^4 \theta$$

$$I_1 = f \sin^2 \theta + g \sin^2 \theta \cos \theta + h \sin^4 \theta$$

The primary advantage of the LADON Facility for these studies is that the polarization of the photon beam can be maintained at 99% over a wide range of photon energies, and much systematic uncertainty in the asymmetry measurement is minimized. Results¹⁰ from the work at LADON are reproduced in Fig. 3. Both the cross sections for unpolarized photons (solid points) and $I_1(\theta)$ tend to be shifted more forward in angle than the theoretical calculations. This discrepancy is particularly acute at the smallest energy of the measurements, 19.8 MeV. The effect of this forward shift is to require a smaller absolute value of the Partovi coefficients, d and g , than predicted,¹¹ and consequently, points to smaller E1-E2 terms in the predicted transition amplitudes.

It is worth noting that results¹² from Argonne indicate the opposite effect below 16 MeV! (See Fig. 4.) Here, the cross sections for the ${}^2\text{H}(\gamma, n)\text{H}$ process were measured relative to that at $\theta_{\text{lab}} = 90^\circ$ and the measured ratio at forward angles is less than the predictions. This would imply that the coefficient d is larger in magnitude than expected below 16 MeV. The reason for either discrepancy is not understood. However, the fact that the Argonne results are in reasonable agreement with the theoretical prediction at 16 MeV and the Frascati work are in disagreement with the calculation at 19.8 MeV suggests that there is an inconsistency between the two data sets.

The photoneutron polarization has been studied extensively below 14 MeV and the results are summarized in Fig. 5. It is surprising that all published measurements¹³ are smaller in magnitude than the calculations¹⁴ which include meson-exchange currents in the M1 component, but agree with the impulse calculation of Partovi. This is another indication that our understanding of the most basic nuclear process, deuteron photodisintegration, is not understood completely even at low energy and further work is necessary.

IV. ELECTRON-DEUTERON SCATTERING

Professor Popov has already introduced¹ the issue of measuring polarization in electron-deuteron elastic scattering. It is now widely recognized that polarization methods provide the only means of isolating the charge and quadrupole form factors for the deuteron. The existing measurements of t_{20} in e-d scattering are shown in Fig. 6. These data represent the entire collection of polarization data presently available in electron scattering studies. The two data points at high momentum transfer were measured¹⁵ with a deuteron tensor polarimeter at the MIT-Bates Laboratory, while the lower q data were determined^{1,16} with an internal polarized target here at Novosibirsk. Clearly, these measurements must be extended to high q^2 and efforts are underway both at MIT and Novosibirsk.

A comparison of the relative scales of these two experiments is indicated schematically in Fig. 7. The experiment at MIT required the use of two large magnetic spectrometers to detect the scattered electrons and deuterons; whereas, the internal target experiment (shown approximately on the same scale in the inset figure) was performed with detector arrays. The Novosibirsk apparatus also is shown with a magnified scale on the same figure so that the individual components can be seen. The detector hardware is

simplified in the internal target geometry because of the purity of the polarized target, the high duty factor of the ring and the low background from the thin internal target.

Of course, the primary limitations of the internal target geometry is the relatively small target thickness, 10^{11} nuclei/cm². Efforts¹⁷ are underway at Argonne to produce a high flux, laser-driven polarized H or D source and to develop a storage cell for the polarized atoms. I shall discuss the recent progress of this work in a few moments. Work is also in progress at Wisconsin¹⁸ to develop storage cells for polarized H or D and much progress has been reported¹⁹ for teflon surfaces. The goal is to produce a polarized target thickness of 10^{14} nuclei/cm² in order to achieve a luminosity of $\gtrsim 10^{32}$ cm⁻² s⁻¹.

V. ELECTRIC FORM FACTOR OF THE NEUTRON

The power of the polarization method is most readily demonstrated²⁰ for measurements of small amplitudes such as the charge form factor of the neutron. The standard Rosenbluth separation is relatively insensitive to the small form factor in this case and the polarization method permits one to observe the product of the charge G_E and magnetic form factors G_M . The expression for the cross section for electron scattering from a free nucleon is given below for an incident electron beam with polarization p_e and a target nucleon of polarization p_N

$$\begin{aligned} \sigma(\theta_e, \theta^*, \phi^*) = & \sigma_M f_{\text{rec}}^{-1} \{ V_L (1+\tau)^2 G_E^2 + 2 V_T \tau (1+\tau) G_M^2 \\ & - 2 p_e p_N [\tau(1+\tau) V_T^1 G_M^2 \cos\theta^* - (2\tau)^{1/2} (1+\tau)^{3/2} V_{TL}^1 G_E G_M \sin\theta^* \cos\phi] \} \end{aligned}$$

where f_{rec} , V 's, τ are defined by Donnelly and Raskin.²¹

Here, θ^* and ϕ^* define the direction of polarization of the target as shown in Fig. 8. Maximum sensitivity to G_E is achieved when $\theta^* = \pi/2$ and $\phi^* = 0, \pi$. Of course, the primary difficulty in performing this experiment is providing the polarized neutron target. The magnitude of the uncertainty in the electric form factor of the neutron can be gauged by the two analyses^{22,23} of data indicated in Fig. 9. In addition to the use of polarized deuterons for this measurement, it has been suggested²⁴ that polarized ^3He would also provide a neutron target since the proton spins are paired off in the S-state of ^3He . R. Milner²⁵ and R. McKeown²⁶ at Caltech have shown that with the advent of new laser technology it should be feasible to fabricate an internal ^3He target of thickness $\gtrsim 10^{15}$ nuclei/cm², and thus, measurements of G_E should be practical. This problem is particularly challenging, however, since longitudinal polarized electrons are required at the target location. Although there are several proposals²⁷ for preserving electron polarization in a ring, there has been no experimental test of these concepts.

VI. INTERNAL TARGET DEVELOPMENT

Now I would like to focus on some recent developments in laser-driven polarized H, D and ^3He targets. A high-flux polarized source of H and D atoms based upon an optical-pumping spin-exchange technique is being developed^{17,28} at Argonne. The method involves a two-step process in which an ensemble of alkali atoms, K say, are polarized by optical pumping and the polarization is transferred to H or D atoms via spin-exchange scattering. This method is attractive since the flux of H or D atoms is limited, in principle, by only available laser power and since the gas load to a storage ring would be minimal.

The primary technical challenge is efficient optical-pumping of the K atoms without the presence of a buffer gas. This means that the spectrum of the laser light must be carefully matched to the Doppler broadened line width of the K atoms and that the surface in the spin-exchange cell must inhibit spin-relaxation of the K and H atoms. The polarization was determined by observing fluorescence from K atoms in the spin-exchange cell when the Zeeman transition frequency for the H atoms was swept with an RF coil. A Breit-Rabi diagram for the H atom is shown in the upper panel of Fig. 10, while the apparatus is shown schematically in the lower half of the figure. If the H atoms are partially polarized we expect to observe two Zeeman transitions in the intermediate magnetic field region. These transitions are observed and shown in Fig. 11. Clearly, the relative intensity of the two transitions reverses as expected between σ^+ and σ^- light. Here we see the first evidence for \vec{H} from an optically-pumped, spin-exchange source! Thus far, a vector polarization of 10% with a flux of $6 \times 10^{16} \text{ s}^{-1}$ for the H atoms has been achieved.²⁸ With the assumption that the H atoms are in equilibrium with the K atoms, and consequently, that the populations $N(m_F)$ of the atoms in H follow a spin-temperature distribution, i.e. $N(m_F) \propto e^{\beta m_F}$ where β is the spin temperature and m_F is the total magnetic quantum number, the polarization of the protons in the spin-exchange cell is found to be 10% from these data. Further improvement in the polarization is expected as we gain more experience with the source. Note that during this experiment only 20 mW of laser power was absorbed in the spin-exchange cell with an H flow rate of 6×10^{16} atoms/s! This is a strong indication that the flux from the source could improve by at least an order of magnitude with a readily available laser power of 0.5 watt.

The goal is to provide a target of D atoms with a thickness of 10^{14} cm^{-2} and a tensor polarization of $t_{20} \gtrsim 0.3$ which could be used in an electron-deuteron scattering experiment. Again, in order to achieve this thickness it is essential to store the atoms in a windowless bottle and permit the atoms to leak away before the spins relax. In order to achieve this goal the high flux and polarization expected from the laser-driven source is essential.

A novel internal polarized ^3He target is being developed²⁹ at Caltech. The ^3He nuclei are polarized by the well-known method of optically-pumping metastable ^3He atoms. This method has benefited recently from the development of lasers which can operate at $1.083 \mu\text{m}$ so that $\gtrsim 3 \times 10^{16}$ $^3\text{He}/\text{s}$ are produced. It is expected that an internal target of ^3He with a thickness of $\gtrsim 10^{15}$ cm^{-2} is feasible.

SUMMARY

It is already clear that photonuclear physics has benefited dramatically from the development of polarized photon sources and that much more work will be performed in the next few years as the new facilities are brought into operation. Electron scattering studies with polarization techniques are potentially a very powerful probe of nucleus and, if development of the methods continues at the present pace, will have a major role in the near future.

This work supported by the U. S. Department of Energy, Nuclear Physics Division, under contract W-31-109-ENG-38.

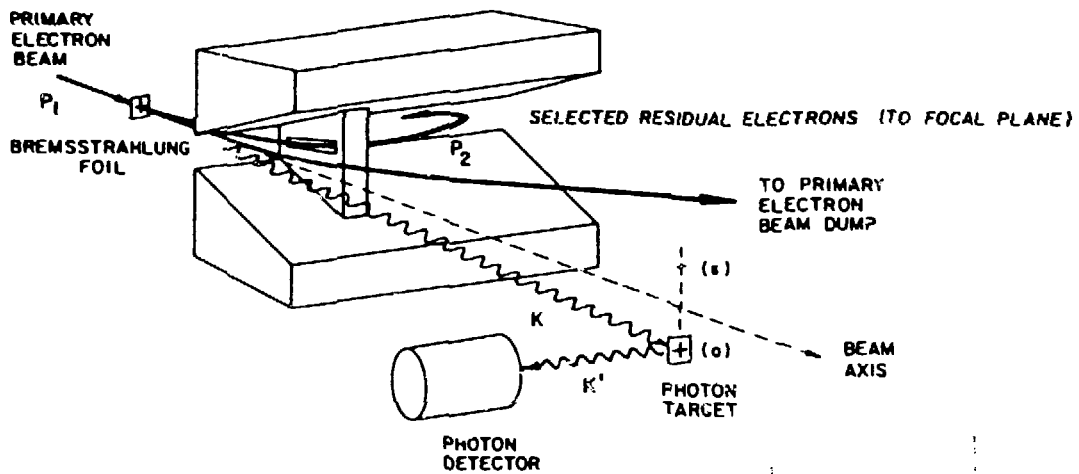
REFERENCES

1. S. G. Popov, the Conference Proceedings.
2. Proc. of the Workshop on Nuclear Physics with the Use of Electron Storage Rings, Lund, Oct. 5-7, 1982, University of Lund Report; Proc. of the Workshop on Polarized Targets in Storage Rings, Argonne, May 17-18, 1984, ANL-84-50; Proc. of the CEBAF Summer Workshop, Newport News, June 25-29, 1984; June 3-7, 1985; Workshop on Polarized Targets: New Techniques and New Physics, Bull. Am. Phys. Soc. 31, 1195 (1986).
3. Proposal for the MIT-Bates Pulse Stretcher Rings, MIT, June 8, 1984; Proc. of the Workshop on Internal Targets and Storage Rings, SLAC, Jan. 1987, to be published.
4. R. J. Holt, Proc. of the Symposium Celebrating 35 Years of Electron Scattering in Nuclear and Particle Science, University of Illinois, Urbana, IL, Oct. 23-24, 1986, to be published; Proc. on Interactions Between Particle and Nuclear Physics, AIP Conf. Proc. No. 123, 499 (1984).
5. R. J. Holt et al., Phys. Rev. C 20, 93 (1979); D. J. Horen, J. A. Harvey and N. W. Hill, Phys. Rev. C 18, 722 (1978); R. Moreh, S. Shlomo and A. Wolf, Phys. Rev. C 2, 1144 (1970).
6. R. M. Laszewski et al., Nucl. Instrum. Meth. 228, 334 (1985).
7. R. M. Laszewski et al., Phys. Rev. Lett. 54, 530 (1985).
8. J. Speth et al., Nucl. Phys. A343, 382 (1980); D. Cha et al., Nucl. Phys. A430, 321 (1984).
9. L. Federici et al., Nuovo Cim. B 59, 247 (1980); M. P. DePascale et al., Appl. Phys. B 28, 151 (1982).
10. M. P. De Pascale, Phys. Rev. C 32, 1830 (1985).
11. F. Partovi, Ann. Phys. 27, 79 (1964).
12. K. Stephenson et al., Phys. Rev. C, to be published.
13. J. P. Sonderstrom and L. D. Knutson, Phys. Rev. C 35, 1246 (1987); R. J. Holt, K. Stephenson and J. R. Specht, Phys. Rev. Lett. 50, 577 (1983); R. Nath, F. W. K. Firk and H. L. Schultz, Nucl. Phys. A194, 49 (1972); W. Bertozzi et al., Phys. Rev. Lett. 10, 106 (1963).
14. E. Hadjimichael, Phys. Lett. 46B, 147 (1973).
15. M. E. Schulze et al., Phys. Rev. Lett. 52, 597 (1984).
16. D. K. Vesnovsky et al., Inst. for Nucl. Phys., Novosibirsk, preprint 86-75.

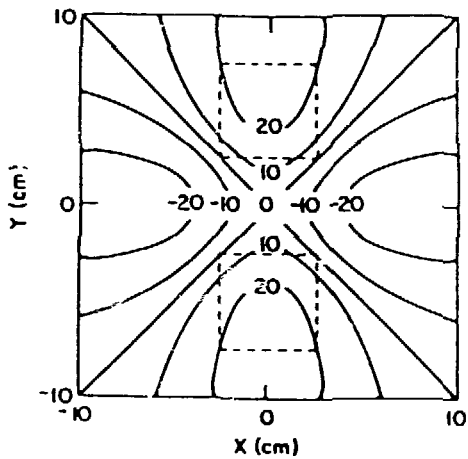
17. R. Holt, Proc. of the Workshop on Polarized Targets in Storage Rings, ANL Report ANL-84-50, p. 103; L. Young et al., Proc. of the Ninth Conf. on Applications of Accelerators in Research and Industry, Denton, TX, Nov. 1986, to be published.
18. W. Haeberli, Bull. Am. Phys. Soc. 31, 1195 (1986).
19. T. Wise, private communication.
20. H. E. Jackson, Proc. of the Workshop on Polarized Targets in Storage Rings, Argonne (1984), ANL Report ANL-84-50, p. 53; M. P. Rekalov, G. I. Gorkh and A. P. Rekalov, Kharkov preprint KFTI 87-I.
21. T. W. Donnelly and A. S. Raskin, Ann. Phys. 169, 247 (1986).
22. S. Galster et al., Nucl. Phys. B32, 221 (1971).
23. M. Gari and W. Krümpelmann, preprint (1986); M. Gari, preprint (1986).
24. B. Blankleider and R. M. Woloshyn, Phys. Rev. C 29, 538 (1984).
25. R. Milner, Proc. of the Workshop on Nuclear Physics Internal Targets, SLAC (1987).
26. R. D. McKeown, *ibid* 25.
27. B. Norum, Report of the 1985 CEBAF Summer Study, Newport News, VA (1985), pp. 17-70.
28. L. Young et al., Bull. Am. Phys. Soc. 32, 1268 (1987).
29. R. G. Milner, R. D. McKeown and C. E. Woodward, Nucl. Instrum. Meth., to be published.

FIGURE CAPTIONS

- Fig. 1 Schematic diagram of the selective-residual electron tagging method is shown in the upper figure. Lower left: distribution of photon polarization at the target position for $E_e = 18.4$ MeV, $E_\gamma = 11.4$ MeV and without selective-residual electron tagging. The target size is given by the dashed lines. Lower right: distribution of photon polarizations with selective-residual-electron tagging. Note the dramatic improvement in the polarization at the target position.
- Fig. 2 Distribution of average $B(M1, \uparrow)$ in ^{206}Pb from Ref. 7 is given in the upper panel. This is compared in the lower panel with the known distribution in ^{208}Pb from Ref. 5.
- Fig. 3 Results from LADON for the $^2\text{H}(\gamma, n)\text{H}$ reaction at four photon energies. The cross section for unpolarized (I_0) and polarized (I_1) photon beam is given. Note that the data at low energy are shifted dramatically toward smaller reaction angles than the calculations.
- Fig. 4 High-accuracy ratios of angular distributions for the $^2\text{H}(\gamma, n)\text{H}$ reaction from Ref. 12. Note that at low photon energy the data are shifted dramatically toward larger reaction angles with respect to the theoretical calculations of Partovi.
- Fig. 5 Summary of the results for the $^2\text{H}(\gamma, n)\text{H}$ reaction below 14 MeV. Surprisingly, the inclusion of meson-exchange currents in the M1 amplitude¹⁴ worsen the agreement between experiment and theory.
- Fig. 6 Summary for all polarization data in electron-deuteron elastic scattering. The two data points at low values of q were determined with an internal polarized target method while the two higher q points were measured with a deuteron polarimeter.
- Fig. 7 Schematic diagram of the apparatus required to measure t_{20} in e-d elastic scattering in the external target geometry. Inset figure on left illustrates the apparatus on approximately the same scale for the internal target experiment at Novosibirsk. The figure is also shown with an expanded scale for ease of identification of the components.
- Fig. 8 Orientation of the spins of the electrons and the nucleon target in electron-nucleon elastic scattering.
- Fig. 9 A comparison of two analyses of the elastic form factor of the neutron.
- Fig. 10 Breit-Rabi diagram for the H atoms indicating the two available Zeeman transitions. The apparatus to induce and detect these Zeeman transitions is illustrated schematically.
- Fig. 11 A comparison of Zeeman transitions for H atoms for σ^+ and σ^- laser light incident on the spin-exchange cell. In this case the H polarization is 10% and the flux is $6 \times 10^{16} \text{ s}^{-1}$. These results represent the first observation of polarized H from a spin-exchange optically-pumped source.



TAGGED BREMSSTRAHLUNG POLARIZATION



TAGGED BREMSSTRAHLUNG POLARIZATION

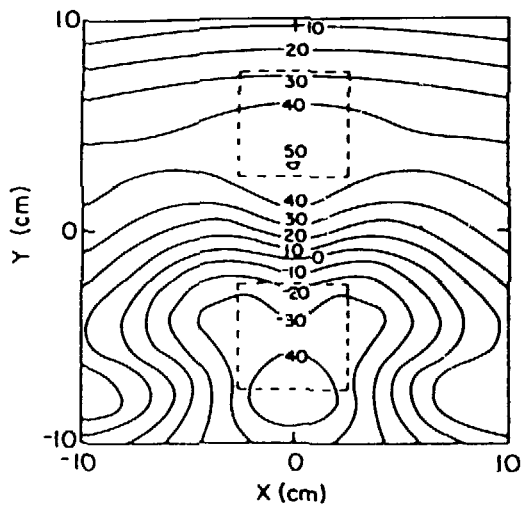


Fig. 1

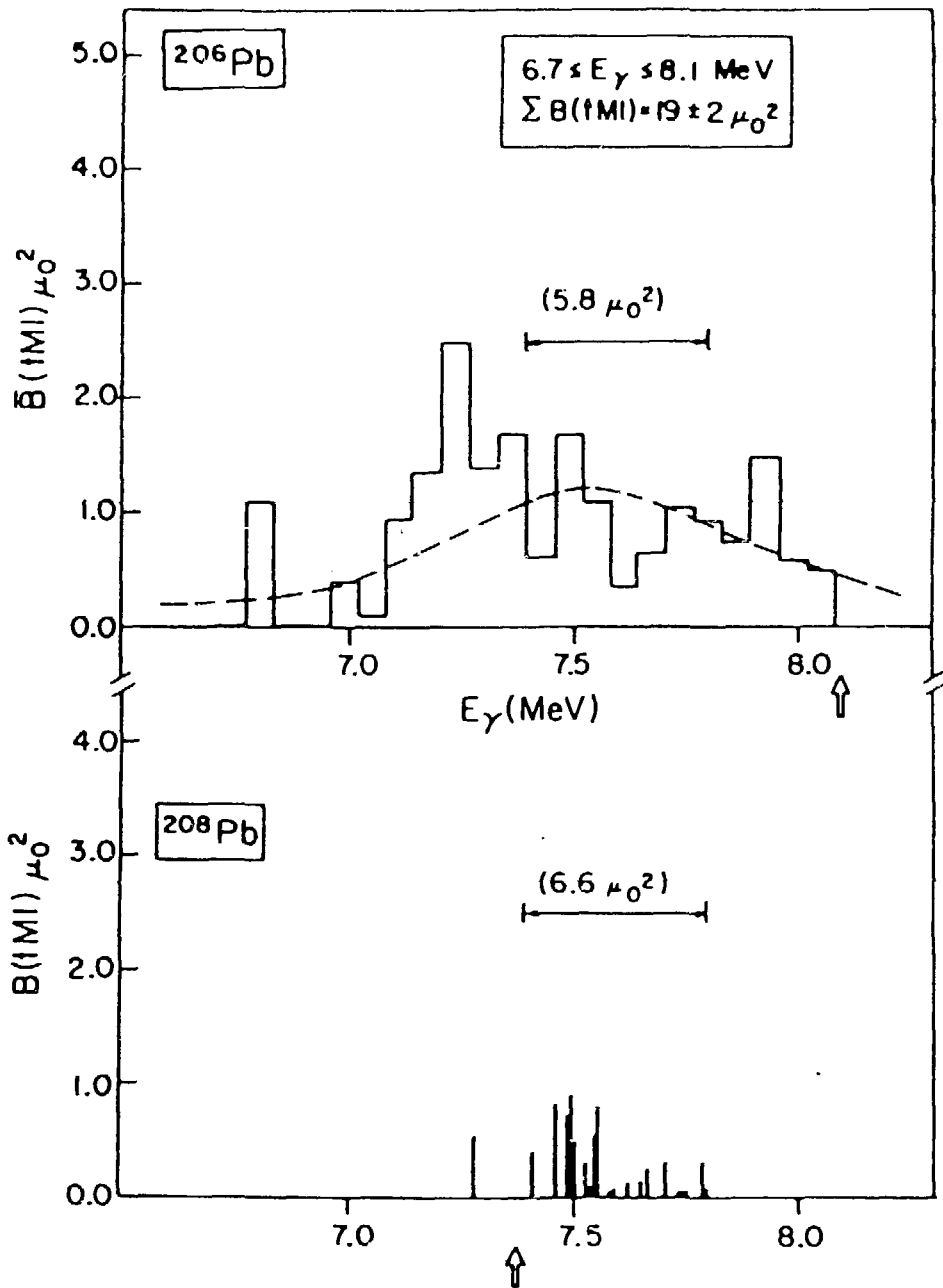


Fig. 2

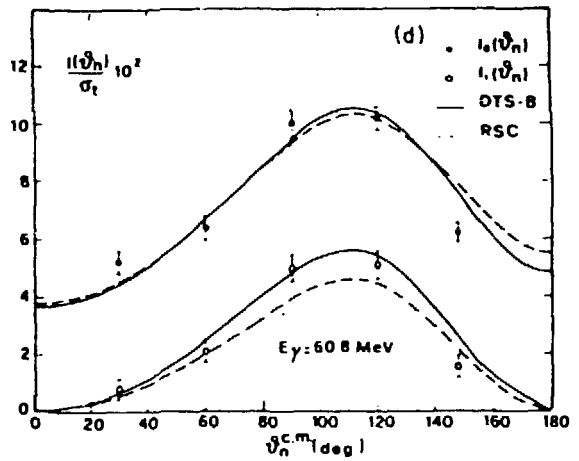
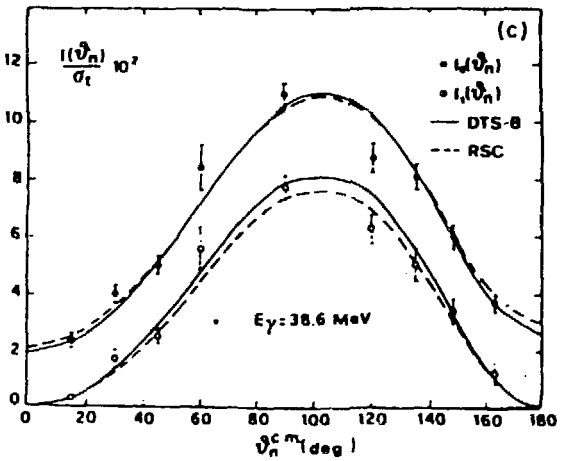
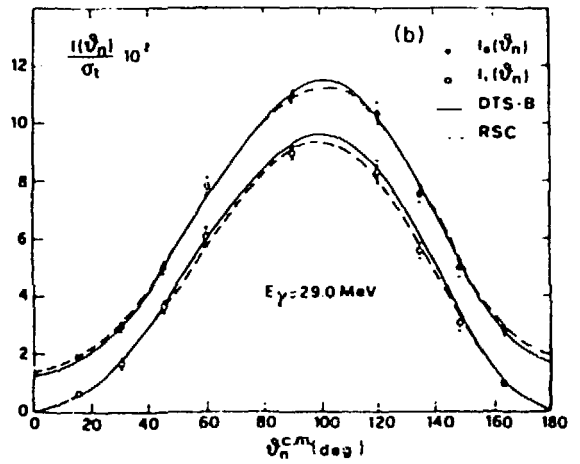
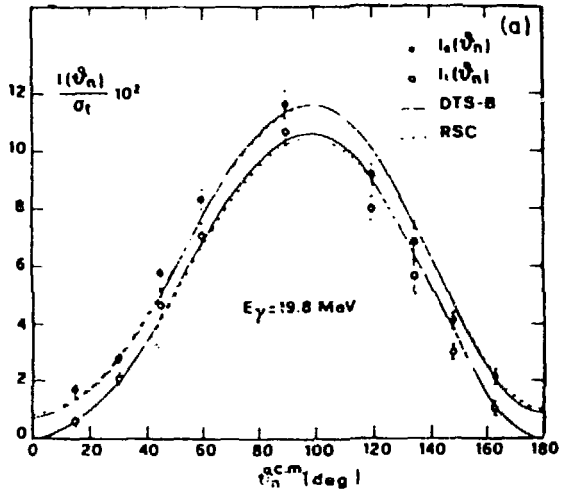


Fig. 3

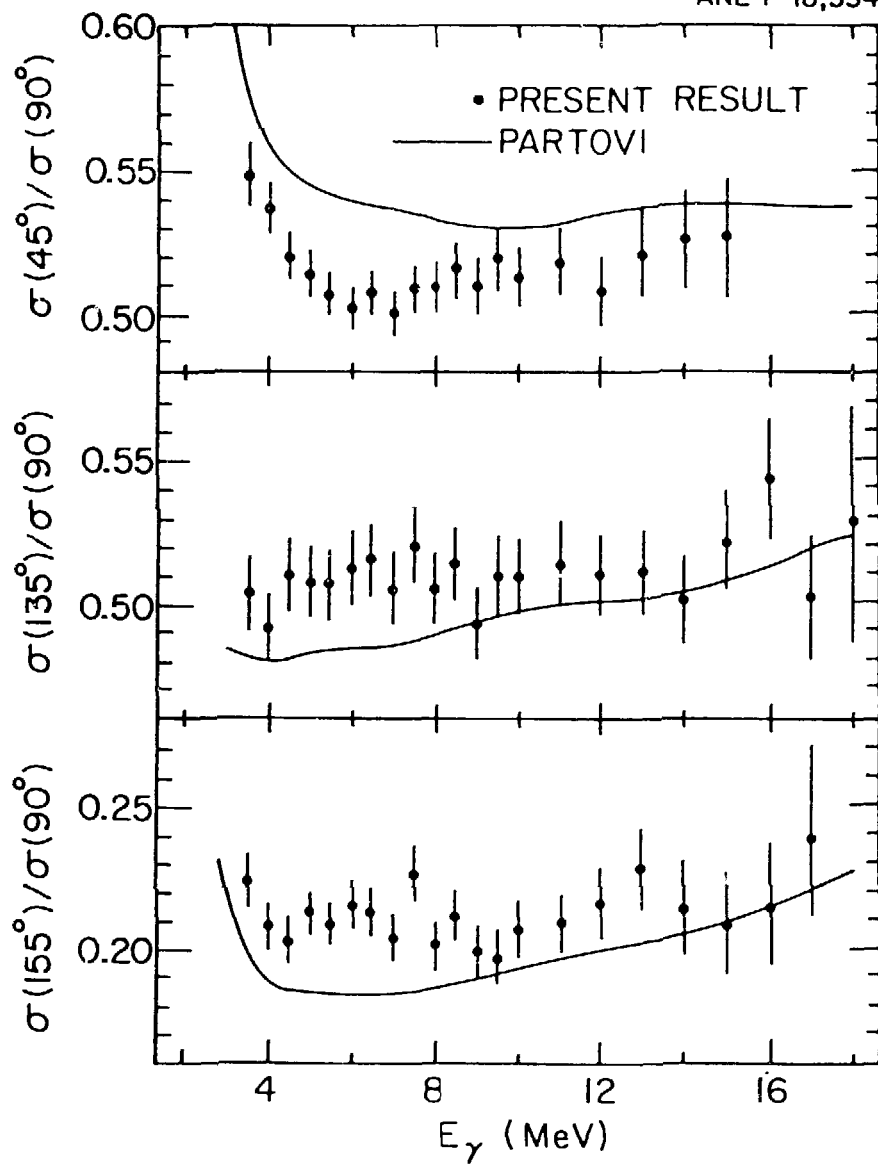


Fig. 4

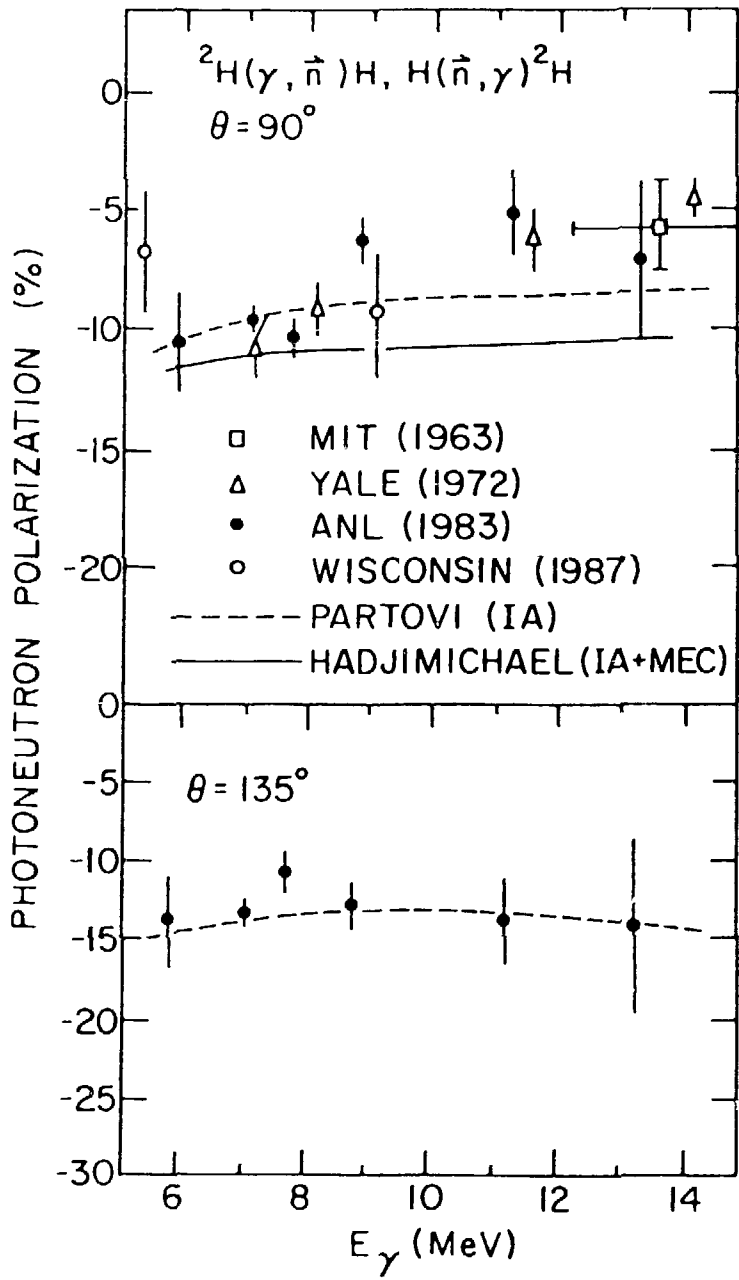


Fig. 5

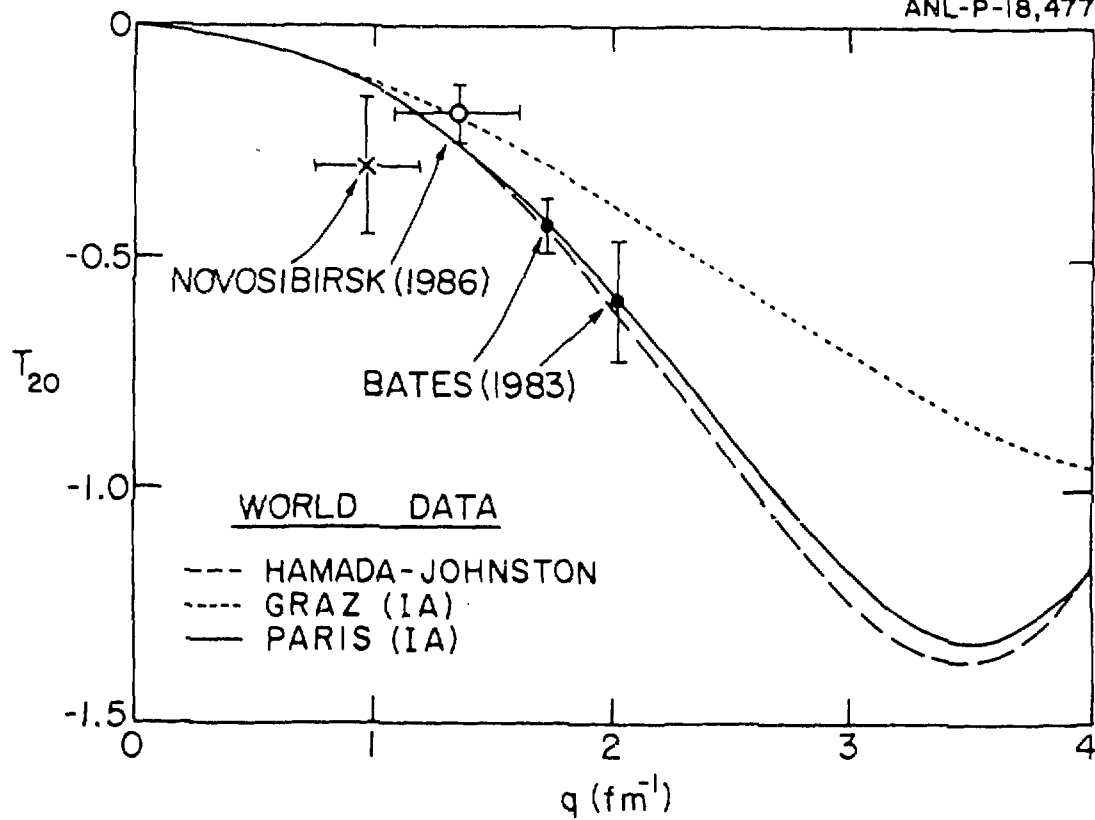


Fig. 6

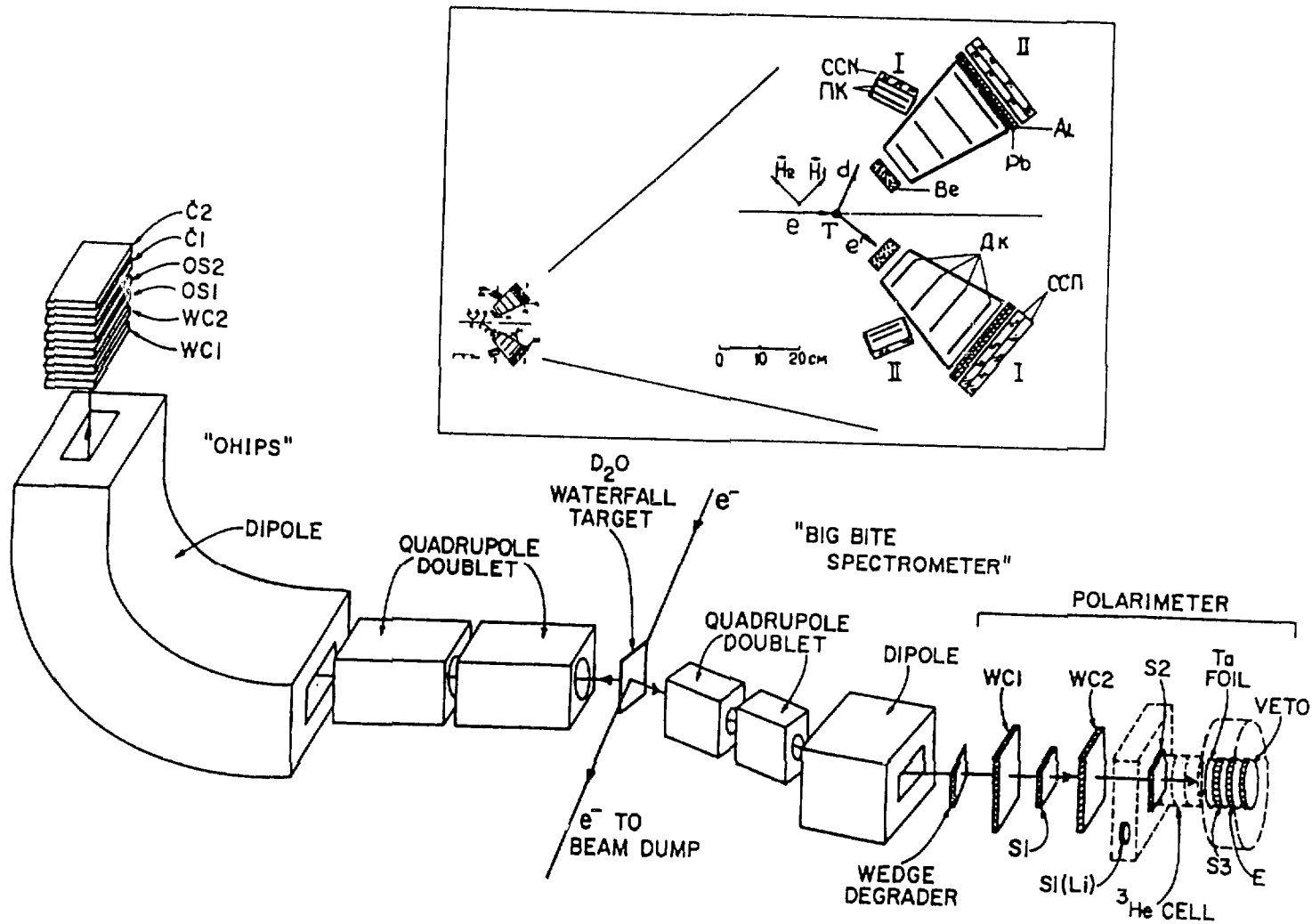


Fig. 7

ANL-P-18,497

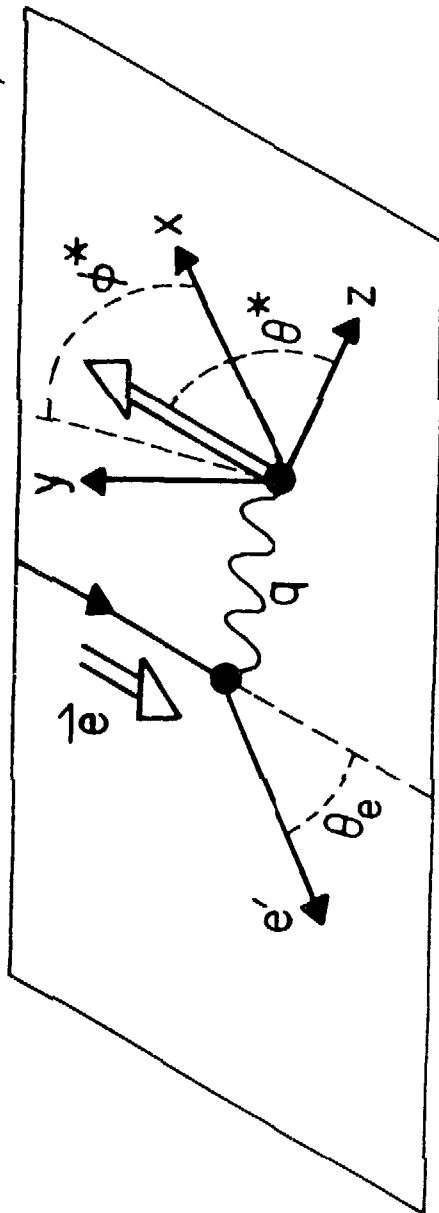


Fig. 8

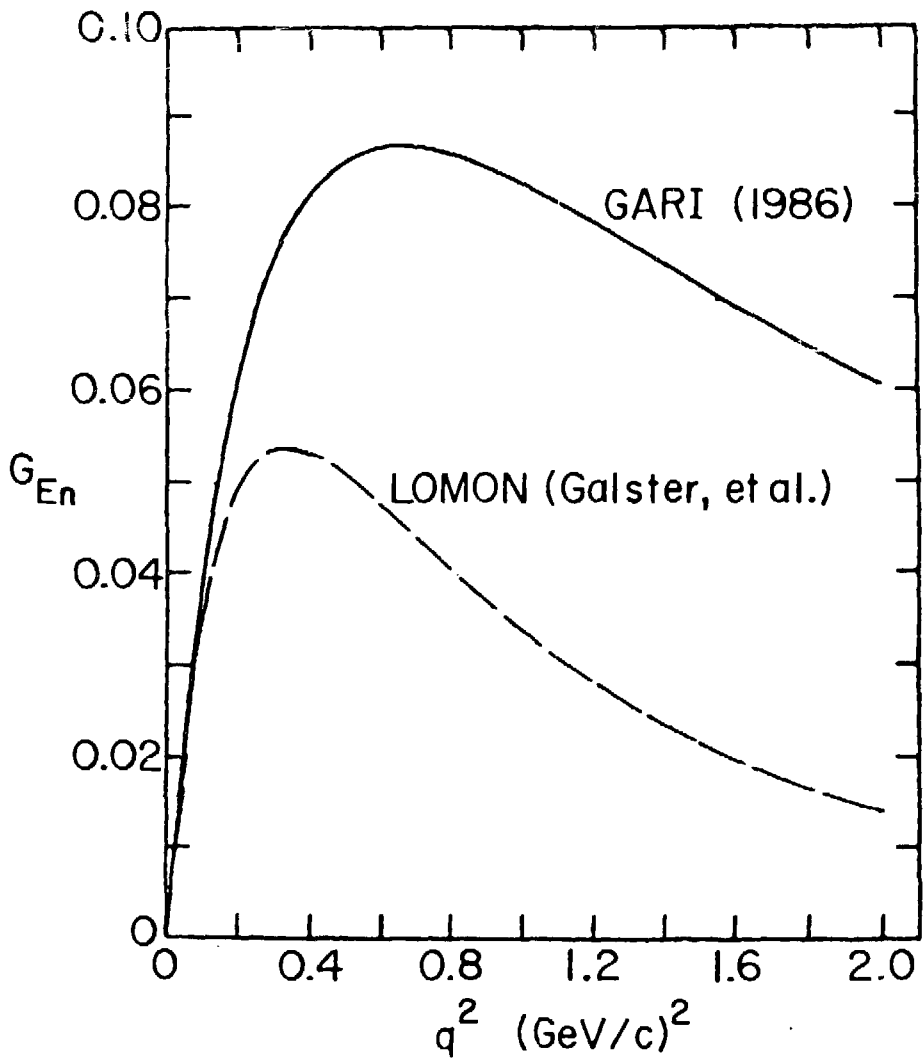


Fig. 9

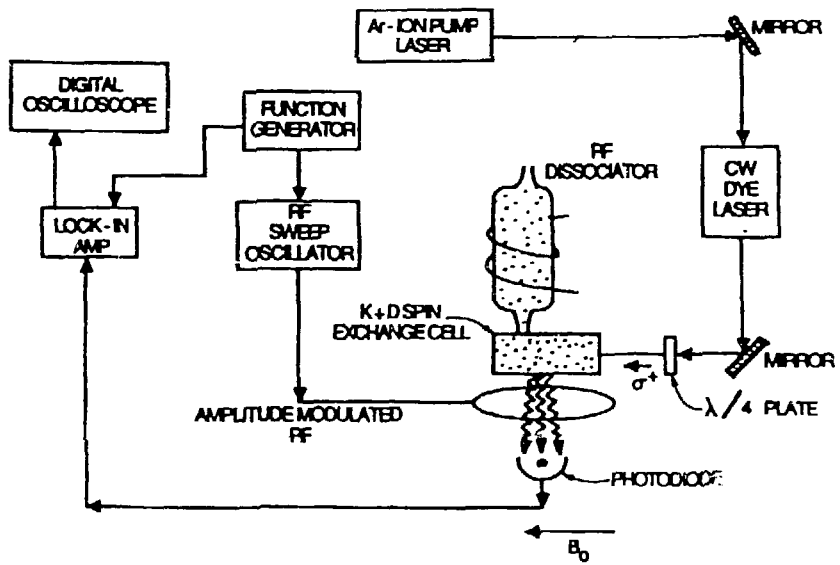
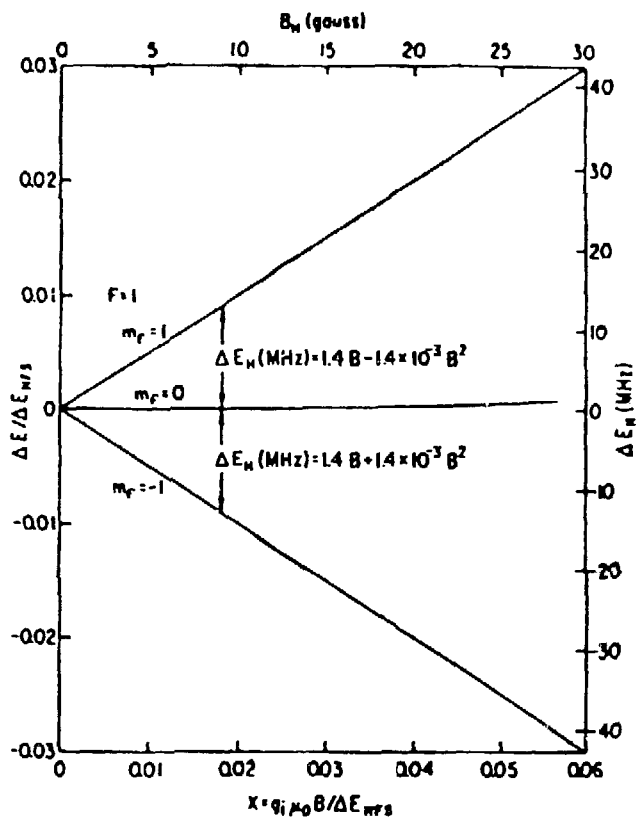


Fig. 10

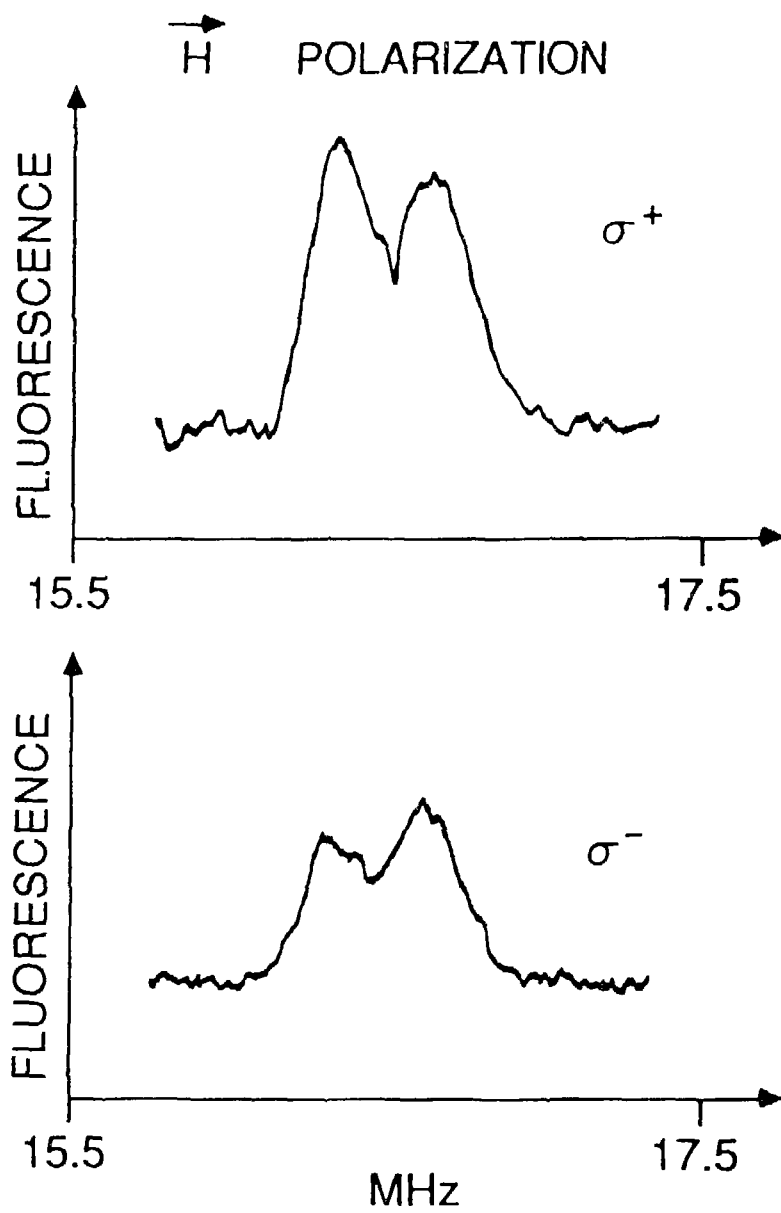


Fig. 11

DISCLAIMER

This report was prepared as an account of work sponsored by an agency of the United States Government. Neither the United States Government nor any agency thereof, nor any of their employees, makes any warranty, express or implied, or assumes any legal liability or responsibility for the accuracy, completeness, or usefulness of any information, apparatus, product, or process disclosed, or represents that its use would not infringe privately owned rights. Reference herein to any specific commercial product, process, or service by trade name, trademark, manufacturer, or otherwise does not necessarily constitute or imply its endorsement, recommendation, or favoring by the United States Government or any agency thereof. The views and opinions of authors expressed herein do not necessarily state or reflect those of the United States Government or any agency thereof.